Bull. Chem. Soc. Ethiop. **2024**, 38(5), 1205-1223.
DOI: https://dx.doi.org/10.4314/bcse.v38i5.2

ISSN 1011-3924
Printed in Ethiopia
Online ISSN 1726-801X

A STABLE ELECTROCHEMICAL SENSOR FOR THE DETECTION OF ASCORBIC ACID BASED ON Fe_3O_4/ZrO_2 NANO COMPOSITE MODIFIED CARBON PASTE ELECTRODE

Genet Bekele[1], Abebaw A. Tsegaye[2*], Abi M. Taddesse[3] and Endale Teju[3]

[1]Department of Chemistry, Injibara University, P.O. Box, 40, Injibara, Ethiopia
[2]Department of Chemistry, Bahir Dar University, P. O. Box.79, Bahir Dar, Ethiopia
[3]Department of Chemistry, Haramaya University, P.O. Box 138, Dire Dawa, Ethiopia

(Received December 8, 2023; Revised May 10, 2024; Accepted May 15, 2024)

ABSTRACT. Magnetite and zirconium oxide (Fe_3O_4/ZrO_2) nano composite, Fe_3O_4 and ZrO_2 nanoparticles were synthesized by a chemical co-precipitation method and hydrothermal decomposition of zirconium metal organic framework, respectively. The structural and morphological properties of the as-synthesized materials were characterized by X-ray diffraction and scanning electron microscope. Electrochemical properties of carbon paste electrode (CPE) modified by Fe_3O_4, ZrO_2 and Fe_3O_4/ZrO_2 nano composites were studied using cyclic voltammetry and electrochemical impedance spectroscopy in the presence of 2 mM $K_3Fe(CN)_6$/0.1 M KCl aqueous solution. Voltammograms acquired on Fe_3O_4/ZrO_2/CPE showed an enhancement of the oxidation current density compared to the other modified electrodes. By applying the Randles-Sevcik equation, the CPE modified by Fe_3O_4/ZrO_2 nano composite resulted in an electroactive surface area of 0.0978 cm^2; about twice to that of the unmodified CPE (0.0458 cm^2). The electrochemical sensor was used for the detection of ascorbic acid (AA). Under optimized condition (pH 4) the sensor exhibits sensitivity of 10 µA/µM; LOD of 0.46 µM; LOQ of 1.53 µM and a linear range of 1-6 µM AA. The Fe_3O_4/ZrO_2/CPE has also shown accepted reproducibility (% recoveries 93.54%); RSD of 2.4% and stable response of 96.91% of the initial current after 30 days of storage.

KEY WORDS: Ascorbic acid, Carbon paste electrode, Electrochemical sensor, Nano composite

INTRODUCTION

L-Ascorbic acid (AA), also known as vitamin C is an organic compound with the molecular formula $C_6H_8O_6$ [1-2]. AA is biologically active; exists as an ascorbate anion in various biological fluids under physiological conditions. It is a water-soluble substance that is essential for all humans. Many natural sources, including fresh fruits and vegetables, provide AA in large quantities. Fruits like oranges, citrus fruits, tomatoes, papaya, pumpkin, and strawberries; fresh vegetables like cabbage, cauliflower, and red and green peppers are the most abundant sources of AA. Ascorbic acid is widely needed for biological processes, in the pharmaceutical industry and in the food industry [1-4]. The role of AA in antioxidant and therapeutic purposes makes it an important food component. The food industry uses AA as an additive, a reducing agent, and stabilizer of the color, taste, and odor of food. Therefore, AA is important for quality control in foods, drinks and used to prolong commercial products' shelf life. This is due to its ability to protect oxidizable constituents by scavenging singlet oxygen, a species that accelerates oxidation reactions [5-8].

The body requires AA mainly a cure for scurvy, anemia, cardiovascular diseases, and *Diabetes mellitus*, and common cold, infectious and liver diseases. It also helps to form collagens protein that has a role to maintain bones, teeth and in wound healing [1, 8, 9]. AA aids the absorption of inorganic iron, lowering the level of plasma cholesterol and prevents the formation of nitrosamine. The biological metabolic activity of folic acid, tryptophan, and tyrosine is also influenced by its role [3]. An AA dose between 0.6 to 2 mg is recommended for proper function of the body [10].

*Corresponding authors. E-mail: abebawadgo@gmail.com

It is also reported that an overdose of AA in some people has side effect such as stomach discomfort, diarrhea, and nausea and skin irritation. Taking AA more than 2 g of body pool inhibits natural processes of its metabolites such as oxalic acid. The loss of taste and aroma in food and beverages may be caused by its excess presence in the body. Therefore, monitoring AA levels in biological fluids has become paramount important. Likewise, ascertainment of AA in medicinal formulations, quality control stage in foods and beverages has given serious attention [11].

Different methods such as chemiluminescence [1, 12], chromatography [13], spectrophotometry [14, 15], and mass spectrometry [16] and flow injection [17, 18] have been used to determine the content of AA in various samples. FTIR-ATR, UV-Vis spectrophotometric and iodimetric titration methods have also been used for the determination of AA in different food, fruit and vegetable samples. For example, Yisak *et al.* [2] reported the content of AA from aqueous extract of white and brown teff grain and in the baked food called injera using iodimetric titration and UV-Vis spectrophotometric methods. Belete *et al.* [3] employed an iodometric titration and UV-Vis spectrophotometric method to measure the level of ascorbic acid and its antioxidant properties in fruits that are available on the market. FTIR-ATR and UV-spectrophotometric methods were also employed by Hagos and co-authors [4] to establish the level of AA in the soluble extracts of pumpkin flesh, peel, and seeds. However, these techniques have some limitations; some of them require expensive instrumentation, long times for analysis and some of them need skilful workers for operation. These drawbacks affirm the need to develop more rapid, sensitive, accurate, simple operation mode and low cost methods such as electro analytical for the determination of AA.

Electroanalytical methods are better than other methods due to their quick analytical responses, high sensitivity, selective determination, low sample requirement, and low power consumption. They are also simple to operate, low cost, reproducible, robust, and are environmental friendly [19]. The working principle in electrochemical methods is that they generally produce electrical signals for example; identified as peak current proportional to the quantity of the target substance that undergoes oxidation or reduction reactions in a selected potential window. The amount of AA in aqueous solution and in solutions which contains both paracetamol and AA were tested using differential pulse voltammetry (DPV) in this study. DPV's advantage in removing charging current allows for accurate determination of small quantities of electro active substances, including AA, using this method. Moreover, its sensitivity is superior to that of the classical cyclic voltammeter methods.

Electrochemical oxidation of AA on unmodified electrodes undergoes an irreversible process. 2,3-Diketogluconic acid is formed during subsequent hydrolysis [20], it is adsorbed at the electrode surface, results electrode fouling and high over-potential requirements. In addition to this, it hampered the reproducibility, selectivity and sensitivity of the electrodes. Moreover, using unmodified electrodes, it is a challenge to selectively oxide AA from biological molecules such as, dopamine and uric acid, since these substances electrochemically oxidize in similar potential window as that of AA. To overcome these problems, use of electrode modified by different materials such as carbon nanotubes [21, 22], graphene [23], ionic liquid [24], conducting polymers [25], metal nanoparticles [26, 27], metal complexes [28, 29] and polymeric films [30, 31] and enzymatic detection [32] have been reported.

Among conventional electrodes, electrochemical quantification of AA content in a sample has been reported using a glassy carbon electrode [33]. Likewise, there are reports in the literature that the amount of AA can be determined utilizing carbon paste electrode (CPE) [34] because of its inherent advantages like low background current and simple renewability of the surface of the electrode. On top of this, fabrication of the carbon paste electrode is easy, it does not require extensive pretreatment, it can be used for longer operational time, and its suitability for modification attracts researchers to use it in a variety of sensing applications. The performance of CPE like selectivity and sensitivity could be enhanced by incorporating various materials as

electrode modifiers in the carbon paste. For example, transition metal oxides, metal nanoparticles and composites have been served as CPE modifiers [6]. Among metal oxides, Fe_3O_4 nanoparticles have attracted many researchers due to their remarkable performance as adsorbents, catalysts and energy storage materials [10]. In addition to this, the magnetite nanoparticles owed additional advantages: low cost, good catalytic performance, easy preparation and compatibility [26, 34].

The fact that as prepared Fe_3O_4 nanoparticles commonly have tendencies to undergo agglomeration and surface oxidation by aging, their performance as electrochemical sensors is hindered significantly. To overcome these shortcomings, preparation of composites of Fe_3O_4 with other nanoparticles using various synthesis protocols in recent years, has led to development of their application in diverse fields. One of the motivating areas of magnetic nanoparticles is their use in electrochemical sensor development. Fe_3O_4 nanoparticle produced by Kingsley *et al.* [34], ZrO_2 nanoparticle synthesized by Baghizadeh *et al*. [35], Fe_3O_4/SiO_2 nano composite formed by Nejad *et al.* [36] and TiO_2/Fe_3O_4 nano composite produced by Jahani and Beitollahi [37] to modify CPE for voltammetry determination of AA is available in the literature. There is still a demand for developing new electrochemical sensors for stable, rapid, precise as well as sensitive determination of AA.

Preparation of magnetite and zirconium oxide nanoparticles has attracted researchers' interest since they have remarkable properties in their catalytic activity; possess a high surface area to volume ratio and their stability for longer times. Fe_3O_4/ZrO_2 nano composite synthesis and applications have been reported to remove nitrate and phosphate ions in aqueous media [38, 39]. As far as our knowledge is concerned, no report in the literature is available detecting electrochemically AA using Fe_3O_4/ZrO_2 nano composite modified CPE. Therefore, this work reports the synthesis of Fe_3O_4/ZrO_2 nano composite for the modification of a bare CPE to be applied as stable electrochemical sensor. Differential pulse voltammetry was used to detect low concentration of AA in solutions and determination of AA in the presence of paracetamol.

EXPERIMENTAL

Instruments

Electrochemical experiments were conducted using Bas100B, USA electrochemical analyzer, a three-electrode cell arrangement. Unmodified and modified CPE (diameter = 3 mm size) as a working electrode, platinum wire as a counter electrode and Ag/AgCl filled internally with 3 M KCl was used as reference electrodes. The X-ray diffraction (XRD) pattern was recorded with XRD (X'Pert ProPANalytical outfitted with an X-ray source of a CuKα radiation having a wavelength of 0.15406 nm. Scanning electron microscope (SEM) (model Hitachi TM1000 with EDX detector) functioning at accelerated voltage of 20 kV was used for morphological analysis of the as synthesized nano composite.

Chemicals and reagents

Ferric chloride hexahydrate ($FeCl_3.6H_2O$, 99%), ferrous chloride tetra hydrate ($FeCl_2.4H_2O$, 99%), zirconium oxychloride octahydrate salt ($ZrOCl_2.8H_2O$, ≥ 95.5%), benzene dicarboxlic acid (H_2BDC, 98%), dimethyl formamide (DMF), methanol (98%), acetic acid, 99.9%, sodium hydroxide, 99%, and hydrochloric acid, 37%, were obtained from Sigma-Aldrich. Potassium chloride, potassium iron(III) hexacynide, 95%, fine graphite powder, 95%, paraffin, 98% collected from Merck, sodium acetate 98%, from BDH and ascorbic acid ($C_6H_8O_6$, 99%) from Blulux laboratories were used as received. AA stock solutions, having a 0.2 M concentration, were prepared in 25 mL of water; 0.88 g of AA powder was dissolved by ultra-sonication. Then, AA solutions of different concentrations (1-6 μM) were prepared using acetate buffer solution. Acetate buffer solution (0.2 M), a supportive electrolyte, was prepared by mixing 8.2 g of sodium

acetate in 5.7 mL of acetic acid into a volumetric flask, 500 mL. The desired pH (2 to 5) value of the buffer solution was adjusted using either 0.2 M CH_3COOH or 0.2 M NaOH. These solutions were kept in a refrigerator at 4 ºC. In the preparation of all solutions, double distilled water was used during the experimental work.

Synthesis of Fe_3O_4, ZrO_2 and Fe_3O_4/ ZrO_2 nano composite

Magnetite was produced by using the chemical co-precipitation method as described in the literature [40]. Stiochiometrical estimated amount of 8.1 g of $FeCl_2.4H_2O$ and 3 g of $FeCl_3.6H_2O$ were dissolved in 100 mL of HCl solution (0.3 M). Subsequently, this solution was added into 120 mL of NaOH (3 M) aqueous solution drop wise over a period of 2 h by constantly stirring at a temperature of 80 ºC under N_2 atmosphere. Meanwhile, the pH of the mixture was kept constant at pH 12 by applying either NaOH or HNO_3 with a concentration of 0.1, 0.01 and 0.001 M solutions. The resulting suspension was left for 4 h to facilitate for the precipitation of a solid at the bottom. Finally, the settled phase, suspension of Fe_3O_4 was washed several times with deionized water and allowed to dry at 60 ºC for 24 h to obtain Fe_3O_4 nanoparticles, which was the desired product.

Nanoparticles of ZrO_2 were prepared from metal organic frame works precursor according to the literature [41]. In a typical synthesis, zirconium oxychloride octahydrate salt 3.94 g is dissolved in 50 mL of DMF and then stirred for 30 min. In another volumetric flask, 2.06 g of H_2BDC was added into 50 mL of DMF, and then the solution was stirred for 30 min to dissolve. Next to this, the metal salt solution was added slowly to the linker solution. These samples were kept in the oven adjusted at a temperature of 120 °C a reaction to proceed for 24 h. After centrifugation at 2500 rpm for 30 min, a precipitate was obtained. The resulting precipitate is sequentially washed three times with DMF and methanol to remove impurities. After the product was dried overnight at room temperature, it was calcined at 500 °C for 6 h to produce ZrO_2 nanoparticles.

The sensing material, Fe_3O_4/ZrO_2 nano composite was prepared with the synthesis protocol Fe and Zr to 75:25 of mole ratio (Scheme 1). First, magnetite suspension was produced using a similar procedure as stated above. In the second step, a magnetite–zirconia oxide nano composite was produced by precipitation of ZrO_2 nanoparticle over the suspension of Fe_3O_4. To obtain the desired product, 1.6 g of $ZrOCl_2.8H_2O$ was dissolved in 100 mL deionized water; the formed solution was added into the Fe_3O_4 suspension. It was followed that the solution was ultrasonicated for 10 min at pH 8, adjusted using either NaOH or HCl with a concentration of 0.1, 0.01 and 0.001 M. Subsequently, it was magnetically stirred for 1.5 h at the temperature of 70 ºC under N_2 atmosphere. Finally, using a permanent magnet, the composite was separated from the solution. After, it was washed several times with deionized water to remove impurities; the product was dried at 60 ºC for 24 h.

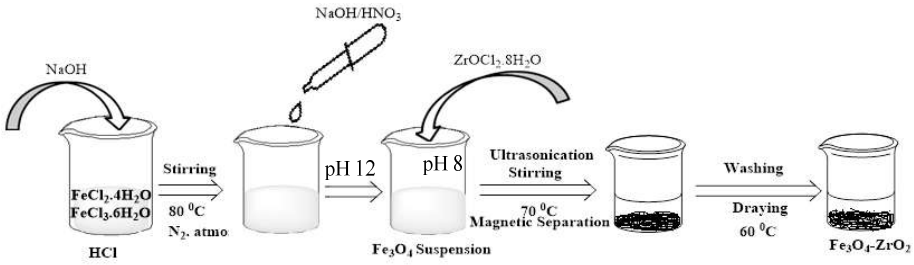

Scheme 2. Synthesis of Fe_3O_4/ZrO_2 nano composite.

Preparation of bare and modified carbon paste electrode

Graphite powder, 5 g and 1.8 mL of paraffin oil as pasting liquid at a ratio of (75:25% w/w) were mixed. First, both components were carefully mixed with a glass rod in mortar. Secondly, it was

rubbed by intense pressing with the pestle. These steps were performed for 30 min to obtain a mixture well homogenized. The paste formed was kept for 24 h for self-homogenization. The ready prepared paste was then packed into a plastic tube (inner diameter of 3 mm). The filling process was made step by step in small portions by pressing closely before adding the next one. Meanwhile, a copper wire was inserted to provide electrical contact. After that, the prepared CPE was left for 12 h before use. The fabricated electrode is made to have a shiny appearance by polishing with paper before utilization. CPE modified by Fe_3O_4/ZrO_2 nano composite was constructed by mixing together graphite (2.01 g), Fe_3O_4/ZrO_2 (0.39 g) and paraffin oil (0.6 g). Next to this, the same steps and procedures listed above to prepare CPE were followed to prepare the proposed sensor for the detection of AA. To compare the performance of the nano composite with that of pristine Fe_3O_4 and ZrO_2 nanoparticles modification of CPE using these materials was performed using the same procedure.

Electrochemical characterization of modified CPE

The electrochemical properties of CPE and modified by Fe_3O_4 and ZrO_2 nanoparticles and their composites were characterized using $K_3[Fe(CN)_6]$/0.1 M KCl as an electrochemical testing material by cyclic voltammetry in potential window from -200 mV to + 600 mV vs. Ag/AgCl reference electrode at various scan rates (10, 25, 50, 75 and 100 mV/s). Moreover, electrochemical impedance spectroscopy (EIS) was used for characterizations of the electrodes by applying a formal potential of $Fe(CN)6^{3-/4-}$, an ac voltage of amplitude of 10 mV and in the frequency range from 1-100 kHz. Electrochemical behavior of AA was investigated using CPE modified by nano materials in 0.2 M acetate buffer solution of pH 4 and at a scan rate of 100 mV/s. Furthermore, the behaviors of $Fe(CN)6^{3-/4-}$ on modified CPE at different scan rates (10 to 100 mV/s) was also conducted using 2 mM AA and pH 4 acetate buffer solution.

The effect of pH on the anodic peak current and peak potential of ascorbic acid was studied during the pH optimization experiment in 0.2 M acetate buffer solution. The pH was varied from 2 to 6 in the presence 2.5 mM AA. The study was performed with CV at a scan rate of 100 mV/s. This study also assisted in assessing proton participation in the electrochemical process, including the proton/electron ratio. Voltammograms of differential pulse voltammetry were recorded using experimental parameters, a pulse potential of 50.0 mV, pulse duration of 50.0 ms and pulse period of 0.2 s in 1 to 6 µM standard solution of AA. Prior to running each experiment, the solutions were bubbled with nitrogen gas (analytically pure with 99.99 %) for 5 min to remove dissolved oxygen. Method validation experiments were also conducted under optimized experimental conditions. All electrochemical experiments were carried out at room temperature.

RESULTS AND DISCUSSION

XRD analysis

The XRD diffraction patterns of the synthesized Fe_3O_4 and ZrO_2 nanoparticles and the binary Fe_3O_4/ZrO_2 system are displayed in Figure 1. The patterns at scattering angles (2θ): 30.6º, 35.5º, 45.0º, 50.2º and 60.3º correspond to the distinguishing characteristic peaks of the tetragonal structure of ZrO_2 nanoparticle (Figure 1a) (JCPDS No. 70-1769). The result indicates ZrO_2 nanoparticle is highly crystalline and different from hydrous zirconia [41]. According to a literature report, the diffraction pattern from 27 to 32º degree contains the strongest line for monoclinic ZrO_2 as well as the tetragonal structure. Even though the tetragonal ZrO_2 phase is expected from ZrO_2 nanoparticles calcined below 500 K, the presence of the monoclinic phase is also evidenced in this work. Zirconia, therefore, exists in this study as a mixture of two phases, the predominant phase being the tetragonal structure.

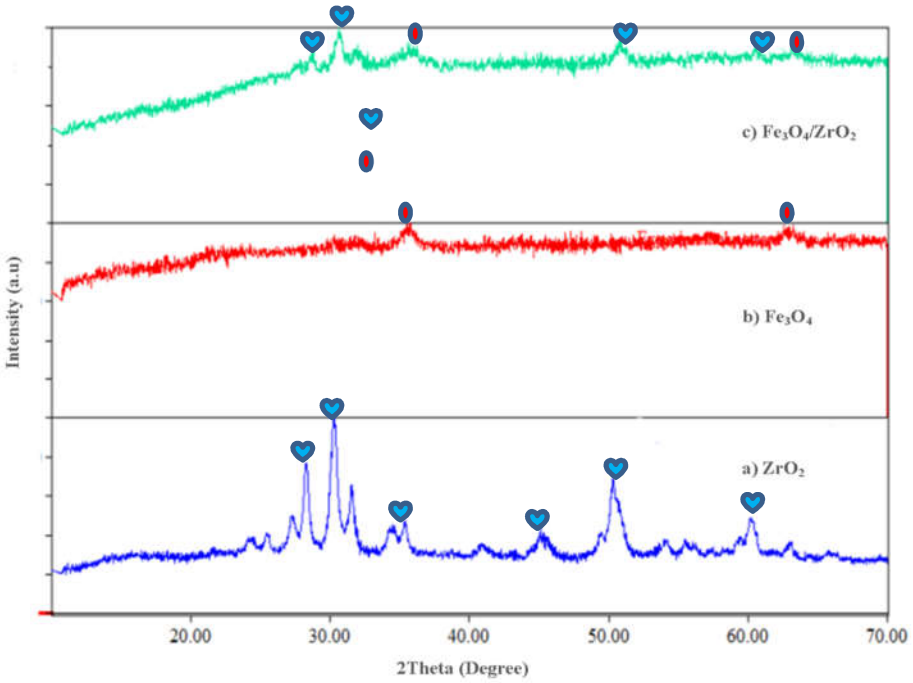

Figure 1. XRD pattern of (a) ZrO_2, (b) Fe_3O_4 and (c) Fe_3O_4/ZrO_2 nano composite.

The diffraction peaks at 2θ = 35.4º and 63.2° are the characteristics peaks normally observed for Fe_3O_4 nanoparticles (Figure 1b) (JCPDS No. 3-0863). In the case of Fe_3O_4/ZrO_2 nano composite the distinguishing diffraction peaks of magnetite and zirconium oxide (28.0º, 30.6º, 50.2º and 60.3º) were demonstrated. Since the composite was not calcined, the peak's intensity decreased compared to the pristine ZrO_2 nanoparticles. It was also noticed that the diffraction at 2θ = 30.3º is due to Fe_3O_4 and ZrO_2 interaction. The crystal size of the nano composite was calculated using the Debye-Scherer equation.

$$D(nm) = \frac{k\lambda}{\beta \cos\theta} \quad (1)$$

where D holds the usual definition of crystal size in nm, k is the Scherer constant (0.89), β which represents the full-width-at-half-maximum of the reflected XRD peak in radians, whereas, λ stands for the wavelength of X-ray (0.15406 nm), and θ half diffraction angle of peak (in degree). The crystalline sizes of Fe_3O_4, ZrO_2 and Fe_3O_4/ZrO_2 nano composite were 9.8, 51.5 and 52.11 nm respectively.

SEM analysis

Figure 2 demonstrates a SEM micrograph and the distribution profile of the elements obtained by EDX for ZrO_2/Fe_3O_4 mixture, Fe_3O_4/ and ZrO_2 nanoparticles. The morphological image appeared to be inhomogeneous, and the nanoparticles were lined up in black with white spots in the case of crystalline ZrO_2 (Figure 2a). The SEM image of the as-synthesized Fe_3O_4 materials (Figure 2b) showed no distinct morphology due to the agglomeration of irregular shaped nanoparticles of different sizes. The morphological image of the composite nanoparticles indicates ZrO_2

nanoparticles are deposited over the agglomerated magnetite nanoparticles (Figure 2c). Figure 2d shows the EDX spectra of the binary composite. The elemental composition showed the amount of Fe in the range from 83.6- 94.8% (average = 88.4%) whereas Zr varied between 5.2 and 16.5% (average = 11.7). The EDX values are not close to the theoretical values we set for the bulk, that is 75% Fe and 25% Zr which revealing the heterogeneity of the binary system. Besides, SEM focuses on elemental composition more on the surface, that the bulk, as the result disparity between values obtained from EDX spectra and bulk is not uncommon.

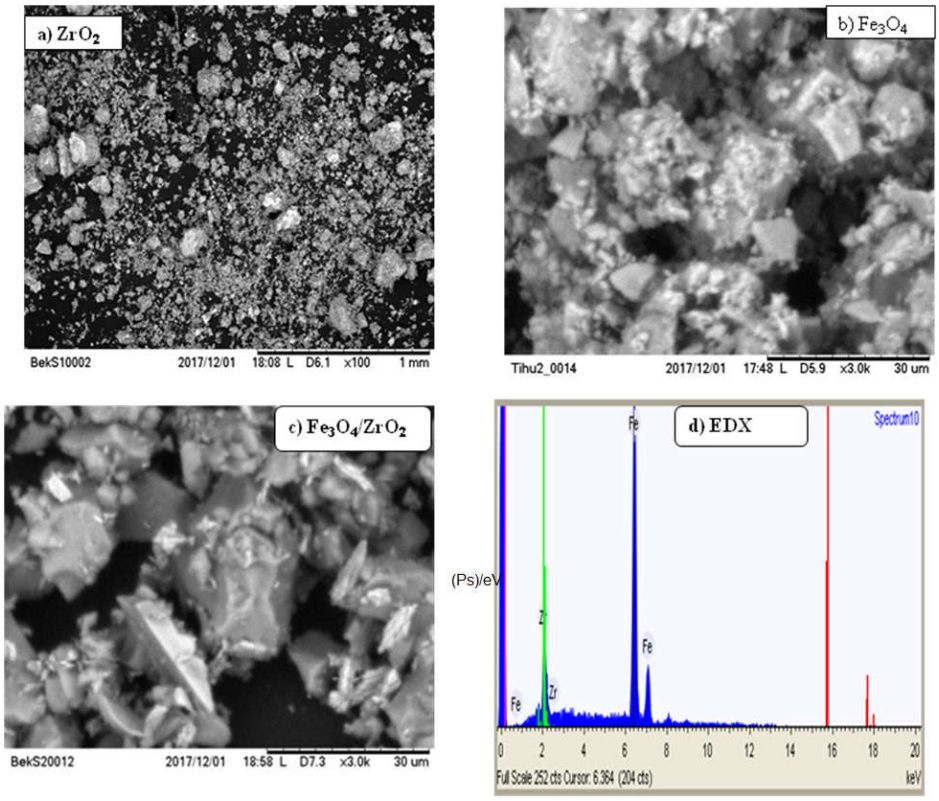

Figure 2. SEM images of a) ZrO_2, b) Fe_3O_4 and c) Fe_3O_4/ZrO_2 and d) EDX spectra of Fe_3O_4/ZrO_2 nano composite.

Electrochemical properties of the modified CPE

Electrochemistry of unmodified and Fe_3O_4/CPE, ZrO_2/CPE and Fe_3O_4/ZrO_2/CPE were characterized using $Fe(CN)_6^{3-/4-}$ (2 mM)/0.1 M KCl as electrohemical probe employing cyclic voltammetry in a potential window from -0.2 to 0.6 V and at various scan rates as of 10 to 100 mV/s. Voltammograms for $Fe(CN)_6^{3-/4-}$ recorded at different electrodes are depicted in (Figure 3a-d). One can see that the intensity of oxidation and reduction peak current of $Fe(CN)_6^{3-/4-}$ at CPE modified by Fe_3O_4/ZrO_2 nano composite increases remarkably by about 10-fold (Figure 3d) in comparison to the other electrodes. It was also found that the anodic peak current of the $Fe(CN)_6^{3-/4-}$ redox system on ZrO_2/CPE was larger than that on Fe_3O_4/CPE and bare CPE (Figure

3a-c). This phenomenon is ascribed to the synergetic effect of increased electrode surface area as shown below and the good electronic conductivity of both ZrO_2 and Fe_3O_4 nanoparticles.

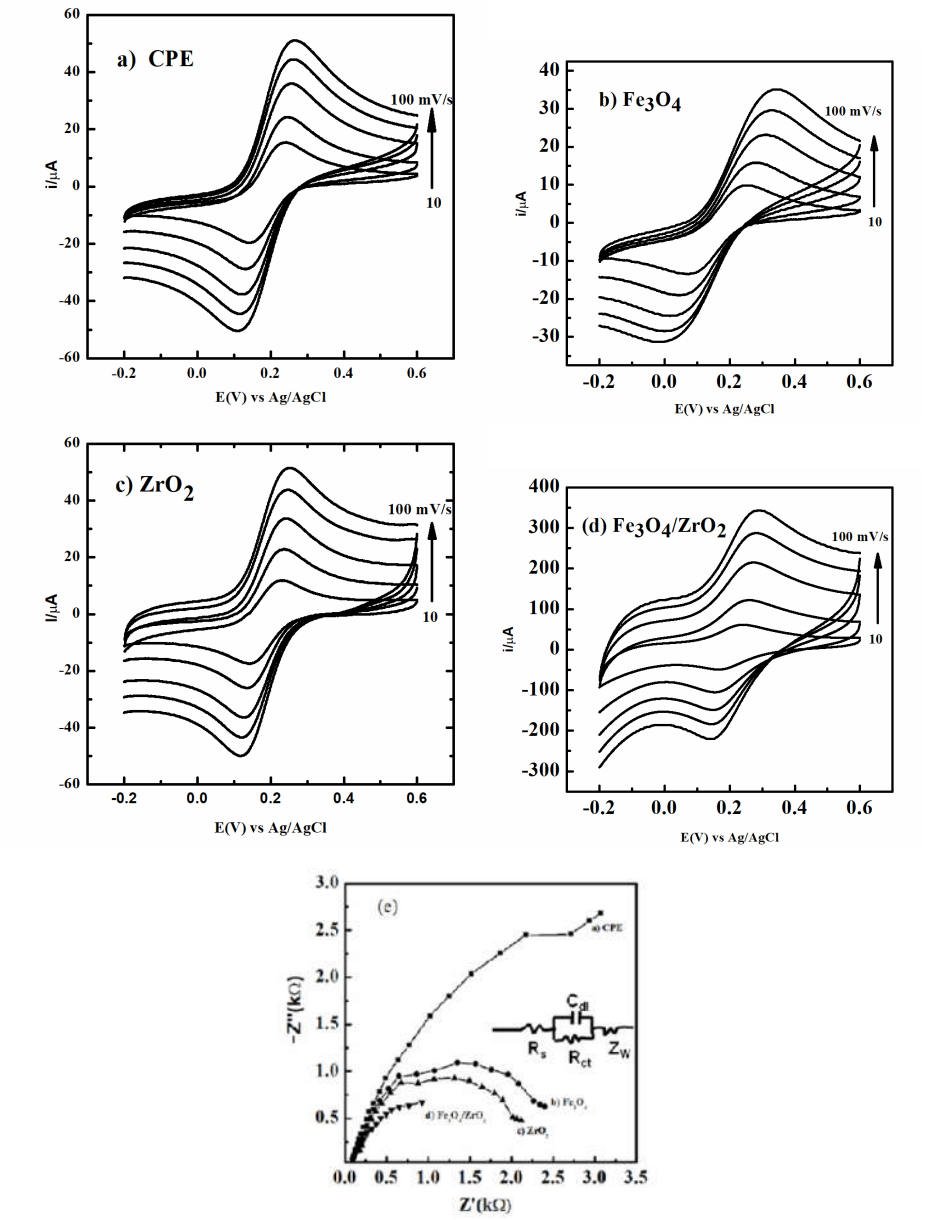

Figure 3. CVs of $Fe(CN)_6^{3-/4-}$ on CPE a) bare, b) modified by Fe_3O_4, c) modified by ZrO_2 and d) modified by Fe_3O_4/ZrO_2 nano composite at scan rates of 10, 25, 50, 75 and 100 mV/s) and (e) Nyquist plot of $Fe(CN)_6^{3-/4-}$ in 0.1 M KCl, (Inset) is an equivalence circuit.

Meanwhile, it was also found that the redox peak potential of $Fe(CN)_6^{3-/4-}$ almost remains constant at lower scan rates on all electrodes. Furthermore, the voltamogram of $Fe(CN)_6^{3-/4-}$ demonstrates an ideal peak-to-peak separation (ΔE_P) potential which occurred in the range of 60 to 80 mV and the ratio of the peak currents are nearly one. These results illustrates the reversibility of the redox probe on various modified CPE.

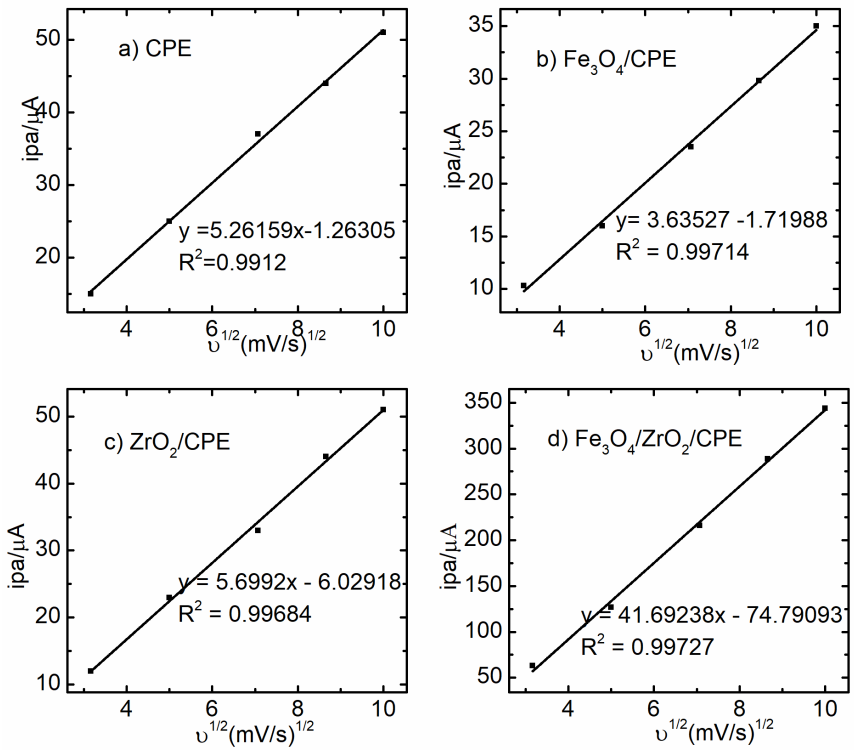

Figure 4. Plot of i_{pa} *vs.* $\upsilon^{1/2}$ of $Fe(CN)_6^{3-/4-}$ on CPE a) bare, b) modified by Fe_3O_4, c) modified by ZrO_2 and d) modified by Fe_3O_4/ZrO_2 nano composite.

Electrochemical impedance spectra of bare and modified CPE were also investigated in the presence of $Fe(CN)_6^{3-/4-}$ as an electro active material in 0.1 M KCl solution by applying an ac amplitude potential 10 mV, formal potential 0.21 V and frequency from 10 to 1000 Hz region.

Figure 3e depicts the EIS spectra of the Nyquist diagrams of $Fe(CN)_6^{3-/4-}$ at CPE (a) and modified by Fe_3O_4 (b), ZrO_2 (c) and Fe_3O_4/ZrO_2 (d). Inset is an equivalent circuit, where, Rs is the solution resistance, R_{ct} is a charge transfer resistance, Z_w is the Warburg impedance and C_{dl} is the double layer capacitance. It was recorded that CPE modified by the binary system gives a small semicircle (R_{ct}) in the high frequency region followed by ZrO_2, Fe_3O_4 and bare CPE. This result manifests the good electrical conductivity of Fe_3O_4 and ZrO_2 nanoparticles that can effectively decrease the charge transfer resistance between the electrode and electro active species. The estimated charge transfer resistance values of the $Fe(CN)_6^{-3/4-}$ redox system at Fe_3O_4/ZrO_2 nanomaterial modified CPE was about 4 times higher (976 Ω) than Fe_3O_4/CPE (2420 Ω) and ZrO_2/CPE (2168 Ω). Low charge transfer resistance implies high conductivity for the magnetite composite consistent to that of the CV results [42].

The Randles-Sevcik equation (2) was applied to estimate the active surface area of both bare and modified CPE.

$$i_{pa} = 2.687 \times 10^5 n^{3/2} A D^{1/2} \upsilon^{1/2} C \quad (2)$$

where n = 1, the number of electrons involved in the redox reaction, A = the area of the electrode given in cm^2, D = 5.15x10^{-6} cm^2/s, the diffusion coefficient of $K_3Fe(CN)_6$ [43], C = 2.0×10^{-3} mol/cm^3, the concentration of $K_3Fe(CN)_6$, and υ is the scan rate in V/s. The plot of i_{pa} *vs.* $\upsilon^{1/2}$ was a straight line with good regression coefficient (Figure 4a-d) indicating the process is diffusion controlled. The active surface area of the electrodes calculated from the slope were 0.0458 cm^2 for bare CPE, 0.046 cm^2 for CPE modified by Fe_3O_4, 0.069 cm^2 for ZrO_2 and 0.0978 cm^2 for Fe_3O_4/ZrO_2. These results indicate that CPE modified using Fe_3O_4/ZrO_2 nano composite electro active surface area was higher by about 2 and 1.5 folds to that of bare and Fe_3O_4 or ZrO_2 modified CPE. The fact that ZrO_2 and Fe_3O_4 nanoparticles characterized by high surface area to volume ratio, there presence in the nano composite enhances the electro active surface area synergistically.

Effect of pH

Ascorbic acid electrochemical behavior is highly influenced by the pH of aqueous solutions. The effect of pH on the electrochemical behavior of AA was investigated by CV at a scan rate of 100 mV/s. The pH of 0.2 M acetate buffer solution was changed from 2 to 6 in the presence of a 2.5 mM standard solution of AA. Figure 5a illustrated voltammograms obtained during the electrochemical oxidation of AA on Fe_3O_4/ZrO2/CPE. The oxidation peak current starts to rise in the initial step with increase in pH until the current reaches the maximum value at pH 4 (Figure 5b). As the pH of the solution increases further, it tends to decrease the height of the anodic wave. This may be due to the existence of unfavorable oxidation kinetics as the result of the repulsive electrostatic interactions between OH anion and ascorbate anion that can further decrease the concentration of AA reaching to the electrode surface. The optimum experimental condition, pH 4.0, was selected for subsequent investigations. Another observation made here was that the anodic peak potential is gradually shifted towards a negative value as the solution pH increased, suggesting the involvement of protons during the AA electrochemical oxidation. The anodic peak potential varies linearly with pH, 0.065 V/pH is the slope of the plot which is close to the ideal value 0.059 for one electron transfer process, demonstrating the involvement of equal numbers of protons and electrons with a ratio 1:1, during the oxidation reaction of AA (Figure 5c). This illustrates that AA proceeded with two step consecutive one electron transfer reaction to form ascorbate radical and dehydroascorbic acid respectively. Scheme 2 shows a net reaction mechanism that demonstrates the oxidation of AA at modified CPE, which is consistent with the literature report [8].

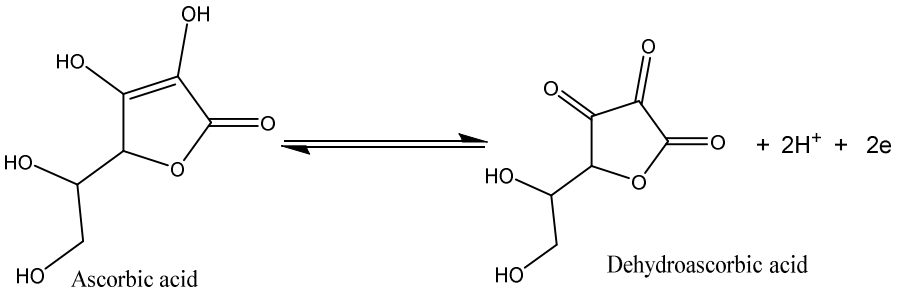

Scheme 2. The proposed reaction mechanism of AA at Fe_3O_4/ZrO_2 modified CPE.

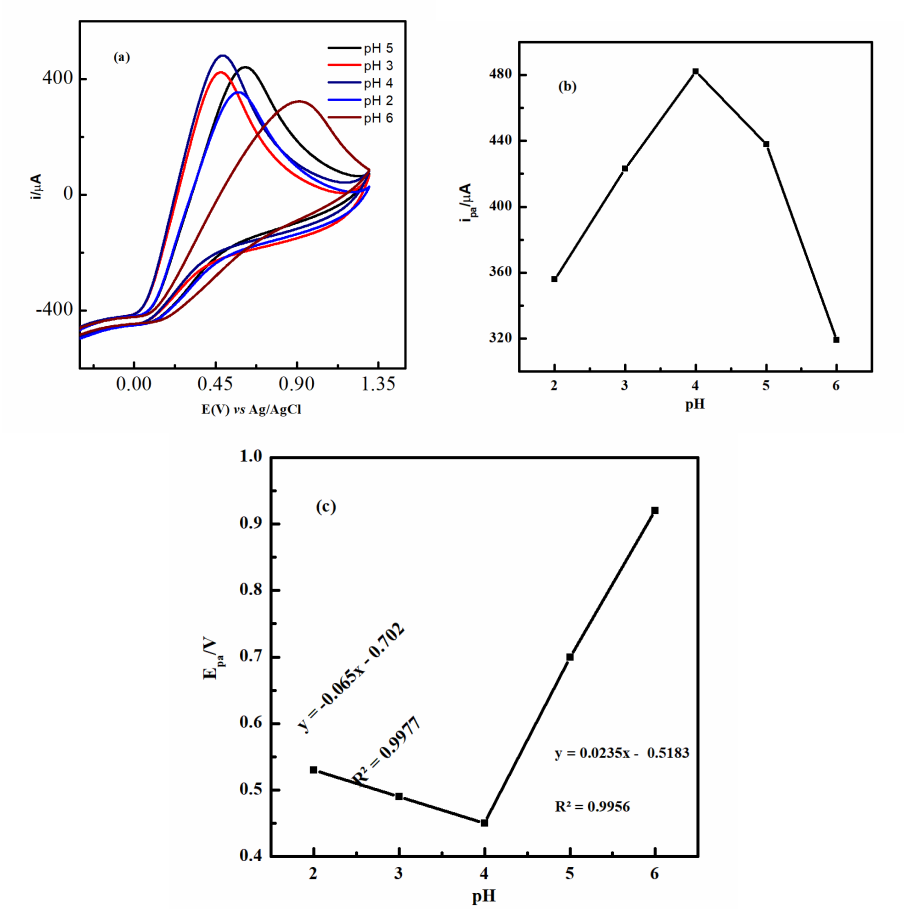

Figure 5. a) CVs obtained on Fe_3O_4/ZrO_2/CPE in 0.2 M acetate buffer in various pH values (2, 3, 4, 5 and 6) in the present of 2.5 mM AA at a scan rate of 100 mV/s; b) plot anodic i_{pa} *vs.* pH of solutions; c) plot of the anodic E_{pa} *vs.* pH of solutions.

Electrochemical behavior of AA at the Fe_3O_4/ZrO_2/CPE

Ascorbic acid is an electro active biological compound. It is oxidized at low potential, and this property motivates researchers to use electrochemical methods for the determination of AA. Ascorbic acid electrochemical oxidation mechanism involves a sequence of steps. In the first step, electrons are transferred reversibly followed by an irreversible chemical reaction. The net overall, reaction is an irreversible process by producing dehydroascorbic acid. During the reaction, an electro-inactive product, 2,3-diketogulonic acid can be produced as dehydroascorbic acid opens the part of lactone's structure. This substance has a tendency to be easily absorbable at the surface of an electrode, which can cause an electrode fouling [10]. In this work, AA (2.5 mM) electrochemical oxidation on Fe_3O_4/ZrO_2/CPE was conducted using cyclic voltammetry and for comparison purpose, AA oxidation on CPE modified by Fe_3O_4 and ZrO_2 particles was also assessed in the acetate buffer solution and at optimum pH 4 and 100 mV/s scan rate.

As seen in Figure 6i(a), AA anodic peak potential was appeared around 0.40 V on bare CPE and the intensity of the peak current was 67 µA. After modification, AA anodic peak potential moved to the negative direction 0.32 V at Fe_3O_4/CPE, 0.24 V at ZrO_2/CPE and 0.20 V at Fe_3O_4/ZrO_2/CPE while the peak current intensity from 160 µA Figure 6i(b), 283 µA Figure 6i(c) and 335 µA Figure 6i(d), respectively. The lowering of onset and peak potential of AA at modified electrodes are attributed to a catalytic property of Fe_3O_4 and ZrO_2 nanoparticles. Equally, at Fe_3O_4/ZrO_2/CPE, AA oxidizes at a potential lower than the others as a result of a synergistic effect of the two oxides in the composite. As can be seen in the voltammograms, the composite modified electrode provided enhanced anodic peak intensity nearly 5 and 2 folds higher than the value of bare and magnetite modified CPE. This may be accounted to the relatively high active surface area of Fe_3O_4/ZrO_2 composite enabling the surface of the electrode to absorb more AA thereby enhancing the signal of AA during oxidation. In all cases, no peak was formed during the cathodic scan, demonstrating the AA oxidation process that follows an irreversible reaction. The oxidation of AA at modified CPE with a considerable shift of oxidation potential towards negative and a remarkable enhancement of the anodic peak current nearly five folds at Fe_3O_4/ZrO_2/CPE could be due to electro catalytic and large surface area of the composite. The result indicates that a synergetic effect of Fe_3O_4 characteristic surface adsorption process [44] and ZrO_2 electro-catalytic nature [45] in significantly improving the electro activity of the electrode toward AA oxidation.

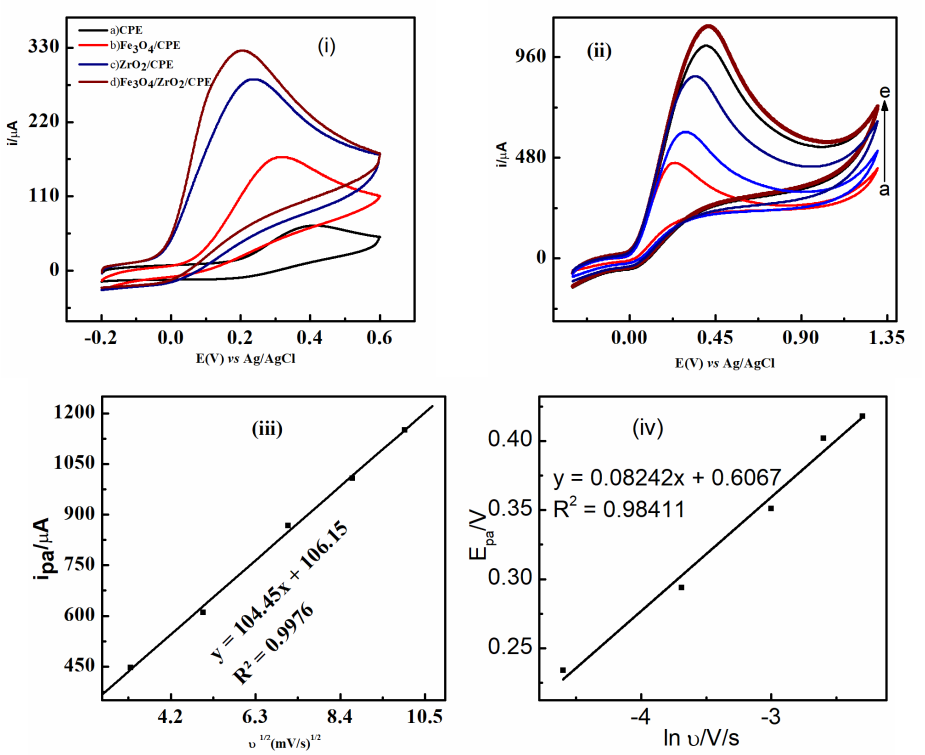

Figure 6. i) CVs of AA (2.5 mM) a) bare CPE, CPE modified by b) Fe_3O_4, c) ZrO_2 and d) Fe_3O_4/ZrO_2, in acetate buffer solution (0.2 M) of pH 4 and at υ = 100 mV/s, ii) CVs of AA (2.5 mM) at CPE modified by Fe_3O_4/ZrO_2 in acetate buffer solution (0.2 M) of pH 4 and at υ = 10, 25, 50, 75 and 100 mV/s), iii) plot of i_{pa} vs. $υ^{1/2}$, iv) plot of E_{pa} vs. ln υ.

Effect of scan rate

The scan rate effects on electrochemical oxidation process of AA (2.5 mM) in acetate buffer supporting electrolyte (0.2 M) was studied using cyclic voltammograms on Fe_3O_4/ZrO_2/CPE. Figure 6(ii) depicts recorded voltammograms at different potential scans (υ = 10, 25, 50, 75 and 100 mV/s). As can be seen from the voltammogram curve, the peak potential becomes more positive as the scan rate is raised indicating an irreversible reaction of AA at the surface of Fe_3O_4/ZrO_2 nano composite. It was also noted that the magnitude of the anodic peak current increased as potential scans were made larger. Plot of peak current (i_{pa}) *vs.* square root of scan rate ($\upsilon^{1/2}$) results in a linear relation as shown (Figure 6(iii)) with a regression equation i_{pa} (μA) = 104.45υ (mV/s)$^{1/2}$ + 106.15 (R^2 = 0.9976). This result confirms that with sufficient over potential, AA oxidation is a diffusion control process.

Kinetic information in the electrochemical oxidation of AA was studied by calculating on electron numbers from the slop of E_p *vs.* lnυ, (Figure 6(iv) a slope of 0.082 V) using Equation 3 for diffusion less process [46]. This result gives a hint that a single electron was involved in the reaction that determines the electrode rate, taking the value of the electron transfer coefficient (α) equal to 0.3.

$$\text{slope} = \frac{\text{RT}}{\alpha n_a \text{F}} \tag{3}$$

In addition to this, equation (4) was used to calculate the product αn_a, where n_a is the number of electrons involved during the electro oxidation step that determines the rate both on unmodified and modified CPE.

$$\alpha n_a = \frac{0.0477}{(E_p - E_{p/2})} \tag{4}$$

where $E_{P/2}$ stands for a potential at the corresponding value to $i_{P/2}$, the oxidation of AA on bare CPE, the product value of αn_a was found to be 0.38 whereas oxidations of AA on CPE modified by Fe_3O_4, ZrO_2, and Fe_3O_4/ZrO_2 nanomaterial were found to be 0.34, 0.29, and 0.20 respectively. These results clearly show that not only electrochemical oxidation of AA peak current is enhanced as a result of modification of CPE by various nano materials, but also a lower required over potential for the electro oxidation of AA at the same electrode surface. This is attributed to Fe_3O_4 and ZrO_2 nano materials synergistically enhancing the catalytic electrochemical oxidation of the AA. Based on this finding and also supported in the literature [36] the mechanism of AA electrochemical oxidation process on Fe_3O_4/CPE surface seems to follow equations (5) and (6). The Fe_3O_4 reduction in the first step produces Fe(II) cations, which are subsequently followed by oxidation to generate Fe(III) cations. This electro catalytic behavior Fe_3O_4 and ZrO_2 nano particles possess (where AA oxidation may be complex) could be the reason for the lower over potential required for the electro oxidation of AA on modified CPE surfaces. The catalytic process involving Fe_3O_4:

$$Fe_3O_4 + 8H^+ + 2e \rightarrow 2Fe^{2+} + 4H_2O \tag{5}$$

$$2Fe^{2+} \rightarrow Fe^{3+} + e \tag{6}$$

Performance of Fe_3O_4/ZrO_2/CPE sensor for the determination of AA

Anodic peak current formed as a result of electro oxidation of AA at Fe_3O_4/ZrO_2, a nano composite modified CPE surface was applied for the detection of AA in aqueous solution. Differential pulse voltammetry (instrumental parameters: 50.0 mV pulse potential, 50.0 millisecond pulse duration and 0.2-s pulse period) was performed under optimized condition pH 4 acetate buffer solution (0.2 M) at potential scan rates of 100 mV/s containing various 1 to 6 μM concentration of AA. The response of Fe_3O_4/ZrO_2/CPE sensor to a range of concentration of AA

is displayed in (Figure 7(a)). The finding indicates that anodic peak current of AA at the surface of the developed sensor was linearity dependent on AA concentration (with a linear regression equation i_{pa}(μA) = 9.91857/(μM/L) - 7.19; correlation coefficient R^2 was found to be 0.9952) (Figure 7(b)). The sensor exhibited good sensitivity of 10 μA/μM; a limit of detection (LOD), 0.46 μM and a limit of quantification (LOQ), 1.53 μM of AA; using LOD = 3α/a and LOQ = 10α/a formula respectively (where 'α' stands for standard deviation of the background current and 'a' is the slope read from the calibration plot).

Table 1 compares the proposed sensor (Fe_3O_4/ZrO_2/CPE) performance with other sensors reported in the literature for the determination of AA. Accordingly, the developed sensor showed lower limit of detection to AA concentration compared to some CPE modified by other materials.

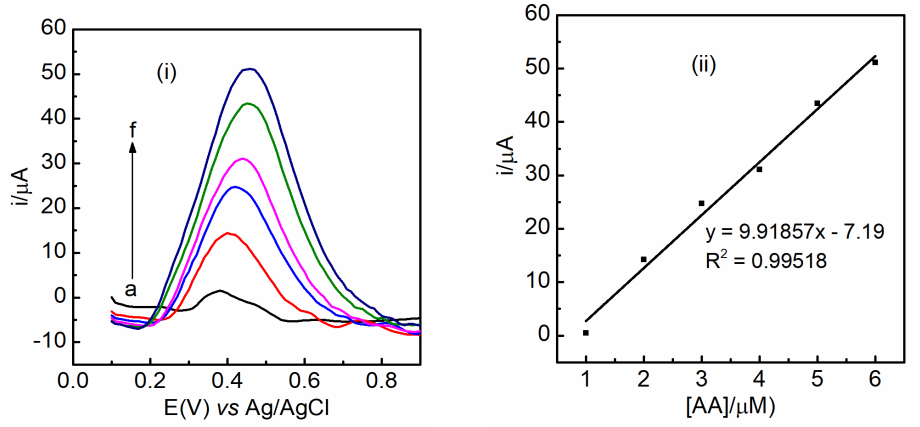

Figure 7. (i) DPVs of AA on Fe_3O_4/ZrO_2/CPE in an acetate buffer solution (0.2 M), pH 4 [(a-f), 1, 2, 3, 4, 5, 6 μM AA] and (b) Plot of i_{pa} *vs.* concentration of AA.

Table 1. Performance of AA sensors constructed using transition metal oxide nanoparticles and composites.

Modified electrodes	Method	Sensitivity ($\mu Amol^{-1}cm^{-2}$)	Linear range (μM)	Lower detection limit (μM)	Reference
Fe_3O_4/CPE	DPV	-	90.9–4700	0.251	[35]
ZrO_2/CPE	SWV		0.07–850	9	[36]
TiO_2/Fe_3O_4/CPE	DPV		2.5–100	0.23	[38]
Fe_3O_4/SiO_2/CPE	DPV		1–900	1.13	[37]
Fe_2O_3/Au film	Amp	1281.9	25–10,000	1	[47]
ZnO-Au/GCE	DPV	264.16	100–4000	4.699	[48]
CdO/SPCE	DPV	420	5–150	0.0535	[49]
Mn-SnO_2	SWV	1092	1–900	0.058	[45]
MnO_2 graphite composite electrode	CV		0–2.5 mol/L	0.4	[50]
Fe_3OZ_4/rO_2/CPE	DPV		1–6	0.46	Present work

Reproducibility, stability and analytical applications

The reproducibility, stability and applications of Fe_3O_4/ZrO_2/CPE sensor were validated by applying DPV and taking repeated five consecutive measurements of AA (2 μM) in acetate buffer

solution (0.2 M). Good in the accepted range, 2.4% relative standard deviation (RSD) was obtained (Table 2). The result confirmed that the proposed method is precise, and it can be applied for assessing the level of AA in various samples including in pharmaceutical drug and biological fluids. Besides, the sensor was able to retain 96.91% of the initial current response after 30 days the electrode was kept at a temperature of 20-22 ºC, this demonstrates that the proposed method was stable (Figure 8).

Table 2. Precision and amount of AA in parcetamol by DPV (n = 5).

Precision

	Standard solution taken (μM)	Mean concentration found (μM)	Apparent % recoveries	%RSD
AA	2.00	1.86	99.91	2.4

Assay of AA in paracetamol

Tablet	Added (μM)	Spiked (μM)	Amount of AA obtained (μM)	% recovery
Paracetamol	1.00	1.09	0.155	93.5

The capability of Fe_3O_4/ZrO_2/CPE for the electrochemical determination of AA in various samples, its performance was verified by assessing the content of AA using DPV under optimum experimental conditions in a solution of paracetamol (2 μM) that contains AA (0.1 μM) in an acetate buffer. Paracetamol tablets used to prepare a solution were purchased from the local market. The result demonstrates that AA was not detected in aliquots of paracetamol sample. The sample was then spiked with 1.0 μM AA known concentration. The calibration curve (Figure 7(ii) was used to calculate the unknown concentration of AA (value of X) using equation y = A + B*X. where A is the intercept and B is the slope and the value of y is the peak current from the recorded DPV measurement for the spiked 1.0 μM AA solution plus the paracetamol sample. Therefore, the amount of AA obtained in paracetamol solution was found to be 0.155 μM (Table 2). The result demonstrates that the AA concentration was slightly larger than that of the expected value, 0.1 μM. This comes about most probably due to the presence of paracetamol, which could bring the matrices effect. Furthermore, satisfactory recovery concentrations of AA in paracetamol (93.54 %) indicate high reproducibility. These values showed that the method developed for the electrochemical detection of AA was precise and also accurate, demonstrating the sensor is appropriate for the determination of AA in various samples as well as in pharmaceutical tablets.

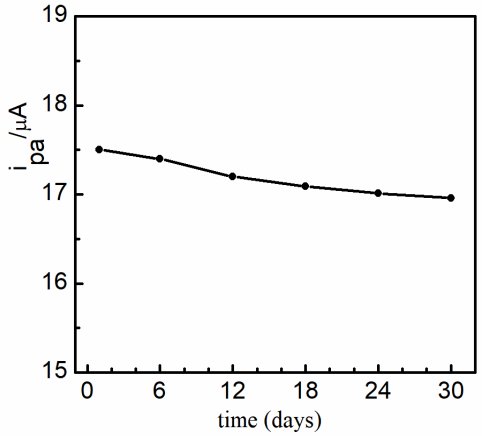

Figure 8. Dependence of peak current with time for 2 μM AA in 0.2 M acetate buffer solution pH 4.

Limitation of the study

This study's capacity to evaluate ascorbic acid in the presence of possible interfering materials and to maximize particular experimental parameters was limited. These affected determining the sensor's selectivity, sorting out the ideal composition ratio for making the best carbon paste electrode and determining the impact of differential pulse voltammetry parameters. In addition, there were time and chemical constraints during the study that prevented a couple of the experiments from being repeated to verify the findings. As a result, some of the plots are reported without showing the margin of error.

CONCLUSION

The Fe_3O_4/ZrO_2 nanomposite was successfully synthesized by a co-precipitation method. Fe_3O_4/ZrO_2 nano composite modified carbon paste electrode was developed for sensing AA. The fact that magnetite has a high absorption capacity together with ZrO_2 high surface area and good catalytic property offered a significant decrease in over potential and improves the electrical signal of AA. The Fe_3O_4/ZrO_2/CPE sensor showed good stability and sensitivity towards electrochemical oxidation of AA. The developed sensor exhibited satisfactory results of with LOD of 0.46 μM. This value is comparable with other electrochemical sensors reported in the literature. Moreover, the Fe_3O_4/ZrO_2/CPE sensor was accurate for determining the concentration AA in paracetamol. Hence, the Fe_3O_4/ZrO_2/CPE sensor may act as a good candidate for sensing AA within various samples.

REFERENCES

1. Caritá, A.C.; Fonseca-Santos, B.; Shultz, J.D.; Michniak-Kohn, B.; Chorilli, M.; Leonardi, G.L. Vitamin C: One compound, several uses. Advances for delivery, efficiency and stability. *Nanomed. Nanotechnol. Biol. Med*. **2020**, 24, 102117.
2. Yisak, H.; Belete, A.; Chandravanshi, B.S.; Redi-Abshiro, M.; Yaya,, E.E. Ascorbic acid content and in vitro antioxidant activities of white and brown teff *[Eragrostictef* (Zucc.)Trotter] grains and injera. *Int. J. Anal. Chem*. **2023**, 2023, 4751207.
3. Belete, A.; Yisak, H.; Chandravanshi, B.S.; Yaya, E.E. Ascorbic acid content and the antioxidant activity of common fruits commercially available in Addis Ababa, Ethiopia. *Bull. Chem. Soc. Ethiop*. **2023**, 37, 277-288.
4. Hagos, M.; Redi-Abshiro; M.; Chandravanshi, B.S.; Yaya, E.E. Development of new analytical methods for the determination of ascorbic acid content in aqueous extracts of flesh peel and seeds of pumpkin (C*ucurbita maxima*). *Bull. Chem. Soc. Ethiop.* **2022**, 36, 277-290.
5. Vazquez, D.; Tascón, M.; Deban, L. Determination of ascorbic acid in commercial juices on a modified carbon paste electrode, by using a Taguchi experimental design. *Food Anal. Methods* **2012**, 5, 441-447.
6. Yang, Y.; Zhou, J.; Zhang, H.; Gai, P.; Zhang, X.; Chen, J. Electrochemical evaluation of total antioxidant capacities in fruit juice based on the guanine/graphene nanoribbon/glassy carbon electrode. *Talanta* 2**013**, 106, 206-211.
7. Padayatty, J.S.; Katz, A.; Wang, H.Y. ; Eck, P.; Kwon, O.; Lee, H.J.; Chen, L.S.; Corpe; Dutta, A.; Dutta, K.S.; Levine, M. Vitamin C as an antioxidant; evaluation of its role in disease prevention. *J. Am. Coll. Nutr.* **2003**, 22, 18-35.
8. Bradshaw, P.M.; Barril, C.; Clark, C.A.; Prenzler, P.D.; Scollary, R.G. Ascorbic acid a review of its chemistry and reactivity in relation to a wine environment. *Crit. Rev. Food Sci. Nutr*. **2011**, 51, 479-498.

9. Zeng, W.; Martinuzzi, F.; MacGregor, A. Development and application of a novel UV method for the analysis of ascorbic acid. *J. Pharm. Biomed. Anal.* **2005**, 36, 1107-1111.
10. Dhara, K; Debiprosad, R.M. Review on nanomaterials-enabled electrochemical sensors for ascorbic acid detection. *Anal. Biochem.* **2019**, 586, 113415.
11. Pisoschi, M.A.; Cheregi, C.M.; Danet, F.A. Total antioxidant capacity of some commercial fruit juices: Electrochemical and spectrophotometrical approaches. *Molecules* **2009**, 14, 480-493.
12. Danet, F.A.; Badea, M.; Aboul-Enein, Y.H. Flow injection system with chemiluminometric detection for enzymatic determination of ascorbic acid. *J. Lumin.* **2000**, 15, 305-309.
13. Dennison, D.B.; Brawley, T.G.; Hunter, G.L.K. Rapid high performance liquid chromatographic determination of ascorbic acid and combined ascorbic acid–dehydroascorbic acid in beverages. *J. Agric. Food Chem.* **1981**, 29, 927-929.
14. Tabata, M.; Morita, H. Spectrophotometric determination of a nanomolar amount of ascorbic acid using its catalytic effect on copper(II) porphyrin formation. *Talanta* **1997**, 44, 151-157.
15. Guclu, K.; Sozgen, K.; Tutem, E.; Ozyurek, M.; Apak, R. Spectrophotometric determination of ascorbic acid using copper(II) neocuproine reagent in beverages and pharmaceuticals. *Talanta* **2005**, 65, 1226-1232.
16. Conley, J.M.; Symes, S.J.; Kindelberger, S.A.; Richards, S.M. Rapid liquid chromatography tandem mass spectrometry method for the determination of a broad mixture of pharmaceuticals in surface water. *J. Chromatogr. A* **2008**, 1185, 206-215.
17. Grudpan, K.; Kamfoo, K.; Jakmunee, J. Flow injection spectrophotometric or conductometric determination of ascorbic acid in a vitamin C tablet using permanganate or ammonia. *Talanta* **1999**, 49, 1023-1026.
18. Nobrega, A.J.; Lopes, S.J. Flow injection spectrophotometric determination of ascorbic acid in pharmaceutical products with the Prussian Blue reaction. *Talanta* **1996**, 43, 971-976.
19. Adane, W.D.; Chandravanshi, B.S.; Tessema, M. Highly sensitive and selective electrochemical sensor for the simultaneous determination of tinidazole and chloramphenicol in food samples (egg, honey and milk). *Sens. Actuators B Chem.* **2023**, 390, 134023.
20. Zen, J.M; Tsai, D.M; Kumar, A.S; Dharuman, V. Amperometric determination of ascorbic acid at a ferricyanide doped Tosflex modified electrode. *Electrochem. Commun.* **2000**, 2, 782 -785.
21. Hu, C.G.; Wang, W.L.; Feng, B.; Wang, H. Simultaneous measurement of dopamine and ascorbic acid at CNT electrode. *Int. J. Mod. Phys.* **2005**, 19, 607-610.
22. Keyvanfard, M.; Shakeri, R.; Karimi-Maleh, H.; Alizad, K. Highly selective and sensitive voltammetric sensor based on modified multiwall carbon nanotube paste electrode for simultaneous determination of ascorbic acid, acetaminophen and tryptophan. *Mater. Sci. Eng.* **2013**, 33, 811-816.
23. Li, F.; Li, J.; Feng, Y.; Yang, L.; Du, Z. Electrochemical behavior of graphene doped carbon paste electrode and its application for sensitive determination of ascorbic acid. *Sens. Actuators B Chem.* **2011**, 157, 110-114.
24. Zhao, Y.; Gao, Y.; Zhan, D.; Hui, H.; Zhao, Q.; Kou, Y.; Shao, Y.; Li. M.; Zhuang, Q.; Zhu, Z. Selective detection of dopamine in the presence of ascorbic acid and uric acid by a carbon nanotubes ionic liquid gel modified electrode. *Talanta* **2005**, 66, 51-57.
25. O'Connell, J.P.; Gormally, C.; Pravda, M.; Guilbault, G.G. Development of an amperometric L-ascorbic acid (vitamin C) sensor based on electropolymerised aniline for pharmaceutical and food analysis. *Anal. Chim. Acta* **2001**, 431, 239-247.
26. Bijad, M.; Karimi-Maleh, H.; Khalilzadeh, M.A. Application of ZnO/CNTs nanocomposite ionic liquid paste electrode as a sensitive voltammetric sensor for determination of ascorbic acid in food samples. *Food Anal. Methods* **2013**, 6, 1639-1647.

27. Chen, X.; Mao, S.S. Titanium dioxide nanomaterials: Synthesis, properties, modifications and applications. *Chem. Rev*. **2007**, 107, 2891-2959.
28. Zhang, Z.J.; Li, X.; Wang, C.G.; Zhang, C.C.; Liu, P.; Fang, T.T.; Xiong, Y.; Xu, W.J. A novel binuclear Schiff-base copper(II) complex modified electrode for ascorbic acid catalytic oxidation and determination. *Dalton Trans.* **2012**, 41, 1252-1258.
29. Karimi-Maleh, H.; Tahernejad-Javazmi, F.; Daryanavard, M.; Hadadzadeh, H.; Ensafi, AA; Abbasghorbani, M. Electrocatalytic and simultaneous determination of ascorbic acid, nicotinamide adenine dinucleotide and folic acid at ruthenium(II) complex ZnO/CNTs nanocomposite modified carbon paste electrode. *Electroanalysis* **2014**, 26 962-970.
30. Silva, F.D.D.; Lopes, C.B.; Kubota, L.T.; Lima, P.R.; Goulart, M.O.F. Polyxanthurenic acid modified electrodes: An amperometric sensor for the simultaneous determination of ascorbic and uric acids. *Sens. Actuators B Chem*. **2012**, 168, 289-296.
31. Vasantha, V.S.; Chen, S.M. Electrocatalysis and simultaneous detection of dopamine and ascorbic acid using poly (3,4-ethylenedioxy) thiophene film modified electrodes. *J. Electroanal. Chem.* **2006**, 592, 77-87.
32. Vermeir, S.; Hertog, M.T.A.L.M.; Schenk, A.; Beullens, K.; Nicolai, M.B; Lammertyn, J. Evaluation and optimization of high-throughput enzymatic assays for fast L-ascorbic acid quantification in fruit and vegetables. *Anal. Chim. Acta* **2008**, 618, 94-101.
33. Wekesa, N.M.N.; Chhabra, S.C.; Thairu, H.M. Determination of L-ascorbic acid in Kenyan fruits and vegetables by differential pulse anodic stripping voltammetry. *Bull. Chem. Soc. Ethiop*. **1996**, 10, 165-169.
34. Svancara, I.; Vytras, K.I.; Barek, J.; Zima, J. Carbon paste electrodes in modern electroanalysis. *Crit. Rev. Anal. Chem.* **2001**, 31, 311-345.
35. Kingsley, M.P.; Desai, P.B.; Srivastava, A.K. Simultaneous electrocatalytic oxidative determination of ascorbic acid and folic acid using Fe_3O_4 nanoparticles modified carbon paste electrode. *J. Electroanal. Chem*. **2015**, 741, 71-79.
36. Baghizadeh, A.; Karimi-Maleh, H.; Khoshnama, Z.; Hassankhani, A.; Abbasghorbani, M. A voltammetric sensor for simultaneous determination of vitamin C and vitamin B_6 in food samples using ZrO_2 nanoparticle/Ionic liquids carbon paste electrode. *Food Anal. Methods* **2015**, 8, 549-557.
37. Nejad, G.F.; Beitollahi, H.; Shakeri, S. Magnetic core shell Fe_3O_4/SiO_2/Graphene nanocomposite modified carbon paste electrode for voltammetric determination of ascorbic acid in the presence of L-cysteine. *Anal. Bioanal. Electrochem*. **2016**, 8, 318-328.
38. Jahani S.; Beitollahi, H. Carbon paste electrode modified with TIO_2/Fe_3O_4/MWCNT nanocomposite and ionic liquids as a voltammetric sensor for sensitive ascorbic acid and tryptophan detection. *Anal. Bioanal. Electrochem.* **2016**, 8, 158-168.
39. Wang, Z.; Xing, M.; Fang, W.; Wu, D. One-step synthesis of magnetite core/zirconia shell nanocomposite for high efficiency removal of phosphate from water. *Appl. Surf .Sci*. **2016**, 366, 67-77.
40. Jiang, H.; Chen, P.; Luo, S.; Tu, X.; Cao, Q.; Shu, M. Synthesis of novel nanocomposite Fe_3O_4/ZrO_2/chitosan and its application for removal of nitrate and phosphate. *Appl. Surf. Sci*. **2013**, 284, 942-949.
41. Silva, G.C.; Luz, I.; Francesc, X.; Corma, A.; Garcia, H. Water stable zirconium benzene dicarboxylate metal-organic frameworks as photocatalysts for hydrogen generation. *Chem. Eur. J.* **2010**, 16, 11133-11138.
42. Lina, X.; Wanga, Y.; Zoua, M.; Lana, T.; Nia, Y. Electrochemical non-enzymatic glucose sensors based on nano-composite of Co3O4 and multiwalled carbon nanotube. *Chin. Chem. Lett.* **2019**, 30, 1157-1160.
43. Miyawaki, O.; Lemuel, B.; Wingard, Jr. Concentration step determination of diffusion and partition coefficients of ferrocyanide for membrane-coated rotating-disk electrode. *Biotechnol. Bioeng*. **1988**, 31, 179-182.

44. Gholivand, B.M.; Torkashvand, M.; Yavari, E. Electrooxidation behavior of warfarin in Fe_3O_4 nanoparticles modified carbon paste electrode and its determination in real samples. *Mater. Sci. Eng. C* **2015**, 48. 235-242.
45. Lavanya, N.; Fazio, E.; Neri, F.; Bonavita, A.; Leonardi, S.G.; Neri, C.; Sekar, C. Electrochemical sensor for simultaneous determination of ascorbic acid, uric acid and folic acid based on Mn-SnO_2 nanoparticles modified glassy carbon electrode. *J. Electroanal. Chem*. **2016**, 770, 23-32
46. Guidelli, R.; Compton, R.G.; Feliu, J.M.; Gileadi, F.; Lipkowski, J.; Schmickler, W.; Trasatti, S. Defining transfer coefficient in electrochemistry: An assessment (IUPAC Technical Report). *Pure Appl. Chem*. **2014**, 86, 245-258.
47. Yin, Y.; Zhao, J.; Qin, I.; Yang, Y.; He, L. Synthesis of an ordered Fe_2O_3/Au film for application in ascorbic acid determination. *RSC Adv*. **2016**, 6, 63358-63364.
48. Hou, C.; Liu, H.; Zhang, D.; Yang, C.; Zhang, M. Synthesis of ZnO nanorodes Au nanoparticles hybrids via in situ plasma spattering assisted method for simultaneous electrochemical sensing of ascorbic and uric acid. *J. Alloy. Compd*. **2016**, 666, 178-184.
49. Gopoalakrishnan, A.; Sha, R.; Vishnu, N.; Kumar, R.; Badhulka, S. Disposal, efficient and highly selective electrochemical sensor based on cadmium oxide nanoparticle decorated screen printed carbon electrode for ascorbic acid determination in fruit juice. *Nano-structures and Nano-Objects*. **2018**, 16, 96-103.
50. Langley, E.C.B.; Clukiz, B.; Banks, E.C.; Compton, G.R. Manganese dioxide graphite composite electrodes: Application to the electroanalysis of hydrogen peroxide, ascorbic acid and nitrite. *Anal. Sci.* **2007**, 23, 165-170.